Title

A novel murine model to deplete hepatic stellate cells uncovers their role in amplifying liver damage in mice

Journal

Hepatology, 57(1)

ISSN

0270-9139

Authors

Puche, Juan E
Lee, Youngmin A
Jiao, Jingjing
et al.

Publication Date

2013

DOI

10.1002/hep.26053

Peer reviewed

Published in final edited form as:
Hepatology. 2013 January ; 57(1): 339–350. doi:10.1002/hep.26053.

A Novel Murine Model to Deplete Hepatic Stellate Cells Uncovers Their Role In Amplifying Liver Damage

Juan E. Puche[1,2], **Youngmin A. Lee**[1], **Jingjing Jiao**[1], **Costica Aloman**[1], **Maria I. Fiel**[1], **Ursula Muñoz**[1,2], **Thomas Kraus**[4], **Tingfang Lee**[1], **Hal F. Yee Jr.**[3], and **Scott L. Friedman**[1]

[1]Division of Liver Diseases, Mount Sinai School of Medicine, NY, USA

[2]University CEU-San Pablo, School of Medicine, Madrid, Spain

[3]Department of Medicine, University of California, San Francisco, CA, USA

[4]Department of Microbiology, Mount Sinai School of Medicine, NY, USA

Abstract

We have developed a novel model for depleting mouse HSCs that has allowed us to clarify their contributions to hepatic injury and fibrosis. Transgenic mice (TG) expressing the herpes simplex virus-Thymidine kinase gene (*HSV-Tk*) driven by the mouse GFAP promoter were used to render proliferating HSCs susceptible to killing in response to ganciclovir (GCV). Effects of GCV were explored in primary HSCs and *in vivo*. Panlobular damage was provoked to maximize HSC depletion by combining carbon tetrachloride (CCl_4) (centrilobular injury) with allyl alcohol (AA) (periportal injury), as well as in a bile duct ligation (BDL) model. Cell depletion *in situ* was quantified using dual-immunofluorescence (IF) for desmin and GFAP. In primary HSCs isolated from both untreated wild type (WT) and TG mice, GCV induced cell death in ~50% of HSCs from TG but not WT mice. In TG mice treated with CCl_4+AA+GCV, there was a significant decrease in GFAP & desmin positive cells compared to WT mice (~65% reduction, $p<0.01$), which was accompanied by a decrease in the expression of HSC activation markers (α-SMA, β-PDGFR and collagen I). Similar results were seen following BDL. Associated with HSC depletion in both fibrosis models, there was marked attenuation of fibrosis and liver injury, as indicated by Sirius Red/Fast Green, H&E quantification and serum ALT/AST. Hepatic expression of IL-10 and IFN-γ was increased following HSC depletion. No toxicity of GCV in either WT or TG mice accounted for the differences in injury.

Conclusion—Activated HSCs significantly amplify the hepatic response to liver injury, further expanding this cell type's repertoire in orchestrating hepatic injury and repair.

Keywords

Herpes simplex virus-Thymidine kinase (HSV-Tk); carbon tetrachloride (CCl_4); fibrosis; apoptosis; bile duct ligation (BDL)

Hepatic stellate cells (HSCs) are well-characterized non-parenchymal cells of the liver with established roles in fibrosis, repair and immunity (1). During liver injury, quiescent HSCs undergo activation, secreting a repertoire of molecules involved in cell proliferation, chemotaxis, inflammation and fibrosis, among others. Although their role in fibrogenesis is

Contact Information: Scott L. Friedman, MD. Division of Liver Diseases. Box 1123, Mount Sinai School of Medicine. 1425 Madison Ave, Rm 1170C. New York, NY 10029, USA Telephone: (001) 212 659 9501 Scott.Friedman@mssm.edu.

Conflict of interest The authors have nothing to disclose.

well established, the contributions of HSCs to acute hepatocellular damage and tissue homeostasis are not well understood.

Models to manipulate HSC function or number offer an appealing strategy to clarify this issue. However, only two models have been established to deplete HSCs *in vivo* thus far, by using gliotoxin (2) or gliotoxin-coupled antibodies against synaptophysin (3, 4). Gliotoxin reportedly induces selective apoptosis of HSCs by subverting NF-κB-mediated survival (2), and can reduce fibrosis and enhance resolution in experimental models, especially when targeted using HSC-specific antibodies (3–5). However, gliotoxin also has broad actions *in vivo* and in culture, targeting not only HSCs but also immune and endothelial cells and hepatocytes (5, 6).

An alternative strategy is to ectopically express the herpes simplex virus-thymidine kinase (*HSV-Tk*) gene in target cells, which renders them susceptible to killing by the antiviral agent ganciclovir (GCV), but only when the cells are proliferating. This possibility was first reported as an anti-cancer approach (7) and further refined (8) in murine sarcoma and lymphoma cells, provoking both apoptotic and non-apoptotic cell death (9, 10). The approach has also been reported in liver injury models and in cultured HSCs (11), but has not been used to deplete HSCs *in vivo* (12).

We have exploited this strategy by using mice expressing the *HSV-Tk* gene driven by the GFAP promoter, which is a marker of HSCs in rodent liver (1). The approach has uncovered a novel and unexpected role for HSCs in amplifying acute liver injury.

Experimental procedures

(Further information is provided in Supplemental Materials and Methods)

Animals

Seven to eight week-old male *Gfap-Tk mice* (B6.Cg-Tg(Gfap-Tk)7.1Mvs/J, Jackson Laboratory, Bar Harbor, ME) were used for *in vivo* experiments in accordance with Institutional Animal Care and Use Committee Protocols. Transgenic mice (TG) express the herpes-simplex virus Thymidine kinase gene (*HSV-Tk*) driven by the mouse glial fibrillary acidic protein (GFAP) promoter. *HSV-Tk* negative littermates served as controls (WT).

In vivo liver injury models for HSC depletion

All treatment schemes are depicted in Supplemental Figure 1. Carbon tetrachloride (CCl_4) and allyl alcohol (AA) were purchased from Sigma-Aldrich (MO, USA). Mice were treated with CCl_4 (0.25 μL/g, i.p. diluted in 50 μL corn oil, on day 1, 4, 7, and 10) and allyl alcohol (0.0125 μL/g i.p. diluted in 100 μL 0.9% NaCl, on day 2, 5, 8) to induce acute liver injury and optimize HSC proliferation while evoking only modest liver damage. To induce selective killing of *HSV-Tk*-expressing HSCs, ganciclovir (GCV) (Cytovene, CA) was administrated from day 3 to day 11 (100 μg/g, i.p. diluted in 0.9% NaCl), n=6.

For bile duct ligation, 8–12 week old mice underwent BDL or sham surgery as previously described (13). WT and TG animals received 100 μg/g/d GCV i.p. diluted in 0.9% NaCl (or 0.9% NaCl alone for sham animals) beginning the day after surgery for 11 consecutive days. At least 5 animals were treated per BDL group (n=5); sham+GCV (n=3), sham+saline (n=2).

Cell lines and cultures

The murine hepatic stellate cell line JS1 has been previously described (14), the mouse hepatocyte cell line AML12 was purchased from ATCC (VA, USA) and the immortalized endothelial cell line TSEC was kindly donated by Vijay Shah, MD (15).

Isolation and culture of primary HSCs and hepatocytes

Mouse HSCs were isolated by in situ perfusion of livers with collagenase and pronase, and Percoll™ gradient centrifugation. Primary hepatocytes were isolated by in situ perfusion with collagenase, followed by differential centrifugation.

Histological analysis

Histological liver analysis performed by an expert pathologist (I.F.) using a score from 0–3 for both centrilobular and parenchymal necrosis, according to the following: 0.None, 1.Isolated hepatocytes, 2.Groups of hepatocytes, 3.Bridging. Ballooning of hepatocytes was scored as follows: 0.None, 1.Mild, 2.Moderate, 3.Severe. For each mouse,10 fields at 100× magnification were analyzed and the average was calculated for each mouse.

Statistical analysis

Unless otherwise stated, data represent mean ± SEM. Statistical analysis was performed by SPSS® software (version 17, IL, USA). Significance was calculated by Student's t-test or, when appropriated, by analysis of variance (ANOVA). Differences were considered significant if $p<0.05$.

Results

Validation of the HSV-Thymidine kinase (HSV-Tk) expression and specific ganciclovir (GCV) toxicity towards cultured primary cells

RT-PCR was performed on mRNA extracted from whole liver and HSCs isolated from both wild type (WT) and *GFAP-HSV-Tk* (TG) mice. Only TG samples consistently expressed the *HSV-Tk* transcript for up to 7 days in primary culture (Supplementary Figure 2A). *HSV-Tk* expression was absent from both WT and TG primary hepatocytes (data not shown).

Optimization of GCV dose in cultured cells

In initial studies, we first established a dose-dependent toxicity curve for GCV in established murine cell lines, and then applied the same concentrations to primary HSCs isolated from WT and TG mice. Both immortalized mouse stellate cells (JS1) cells and hepatocytes (AML12) were incubated with incremental GCV concentrations for 3 days. GCV-mediated toxicity unrelated to *HSV-Tk* gene expression was analyzed by assessing ^{3}H-thymidine incorporation, and AlamarBlue Assay. Cell death was determined by staining with trypan blue and determining the percentage of viable cells. Using this approach, GCV doses higher than 10 μM were toxic in cell lines (Supplementary Figure 2B–D), and subsequent experiments in primary cells therefore used 5 μM GCV, which avoided non-specific toxicity.

Next, primary HSCs from both WT and TG mice were cultured for 5 days with GCV (5 μM and 500 μM) or saline. Specific GCV toxicity was determined by measuring ^{3}H-thymidine incorporation and trypan blue staining (Figure 1A, B). Only TG HSCs exhibited significantly decreased thymidine incorporation and cell survival, indicating specific GCV-mediated killing at 5 μM, thus validating the construct for use *in vivo*.

To further establish the specificity of GCV, we also isolated primary hepatocytes from both WT and TG mice, incubating them with GCV at the same concentrations (5 μM and 500 μM). In primary hepatocytes, 5 μM GCV had no impact on the cells, whereas 500 μM GCV remained toxic, highlighting the specificity of cell killing at the 5 μM concentration (Supplementary Figure 2E). Immortalized endothelial cells (TSEC) treated with the same GCV doses behaved identically to primary hepatocytes, with no decrease in ^{3}H-thymidine incorporation at 5 μM GCV but a significant effect at 500 μM (Supplementary Figure 2F).

GCV kills HSV-Tk-expressing HSCs by apoptosis

We next determined the mechanism underlying the GCV-mediated killing of TG HSCs by measuring PARP cleavage by Western blot as a reflection of apoptosis. Using this approach, only TG HSCs treated with GCV displayed specific PARP cleavage (Figure 1C). Transgenic HSC killing was also completely inhibited by the pan-caspase inhibitor z-VAD-fmx, further establishing apoptosis as the underlying mechanism of GCV-mediated killing (Figure 1D).

Optimization of HSC depletion in vivo following GCV administration

We next established the specificity of GCV effects *in vivo*. A dose range was performed by administering GCV in different concentrations (20–150 μg/g body weight), ip daily for up to 10 days in WT and TG mice. None of these mice displayed behavioral or morphological changes (data not shown), or any increase in serum ALT levels (Supplementary Figure 3A). In contrast, more prolonged treatments using higher doses of GCV (≥150 μg/g) led to a significant decrease in weight in TG, but not WT mice (Supplementary Figure 3B). This finding, together with previously published studies (16), led us to choose a final dose of 100 μg/g in subsequent experiments to deplete TG HSCs *in vivo*.

Because HSCs must be proliferating to render them susceptible to GCV-mediated killing, we next optimized the method of liver injury required to maximize HSC depletion. To do so, we used CCl_4 and allyl alcohol (AA) to induce selective injury to the centrilobular and periportal regions, respectively. Accordingly, we performed a dose-dependent toxicity curve after 4 doses of AA (every 3 days) choosing 0.0125 μL/g as the final dose, based on mouse survival, the extent of HSC activation (α-SMA IHC) and liver damage (H&E), to provoke the most widespread HSC proliferation while minimizing hepatocyte damage (Supplementary Figure 4). A dose of 0.25 μL/g CCl_4 in 50 μL oil was used to optimize centrilobular HSC activation. The treatment scheme is depicted in Supplemental Figure 1A.

Validation of HSC depletion in TG mice

In TG mice treated with CCl_4+AA+GCV ("depletion treatment"), there was a significant decrease of desmin and GFAP co-expressing cells with a reduction of ~65%, $p<0.01$ as assessed by immunofluorescence co-localization analysis compared to WT mice receiving the same treatment (Figure 2A and Supplementary Figure 5). This decrease in protein expression was accompanied by a reduction of *GFAP* mRNA in mice undergoing HSC depletion (Figure 2B).

To further analyze the efficacy of the depletion treatment, we assessed markers of HSC activation, including α-SMA immunohistochemistry, and β-*PDGFR* and *collagen I* mRNA quantification. Figure 3A displays a >90% depletion of α-SMA positive cells in TG animals with HSC depletion, compared to WT mice. Consistently, β-*PDGFR* and *collagen I* mRNA expression levels were decreased in TG mice following HSC depletion, compared to WT mice (Figure 3B). Of interest, *CXCR4* has been recently implicated in HSC activation (17), and its mRNA expression in TG mice undergoing HSC depletion was also reduced (Figure 3C).

We confirmed these findings in a bile duct ligation (BDL) model. BDL (or sham) was performed in WT and Tg mice (n=5) (Supplementary Figure 1B). Mice received 100 μg/g/d GCV ip. (or 0.9% NaCl) for 11 days. In Tg mice that had been treated by BDL+GCV, desmin positive cells were significantly decreased compared to WT mice, indicating that activated GFAP-expressing fibrogenic cells proliferate following BDL as well, and that these cells can therefore be successfully depleted in BDL by GCV in *Gfap-HSV-Tk+* mice (Supplementary Figure 6).

To determine if apoptosis accounted for HSC depletion *in vivo* as in culture, we performed TUNEL staining in mice that had been treated with CCl_4+AA+GCV for 4 days instead of 10 days, since we expected the number of HSCs undergoing apoptosis to be higher at this time point. Indeed, at 4 and 7 days, HSC depletion was evident (reduction of ~ 40% and 50%, respectively, $p<0.05$) albeit to a lower extent (Supplementary Figure 7). As anticipated, a significant increase in non-parenchymal TUNEL-positive cells was evident in TG mice compared to WT animals after the depletion treatment (Supplementary Figure 8A). To further establish that these non-parenchymal TUNEL positive cells were HSCs, we analyzed serial sections with staining for TUNEL and desmin (Supplementary Figure 8B), which demonstrated apparent expression by the same cells, although double immunofluorescence and confocal microscopy would be required for strict confirmation of co-expression.

Of interest, HSC depletion with CCl_4+AA+GCV was not accompanied by any detectable non-liver effects of GCV on other GFAP-expressing populations. Specifically, there were no differences in animal behavior, survival at 30 days, leukocyte counts, serum creatinine, Cyp2E1 activity (which metabolizes CCl_4 and allyl alcohol) (Supplementary Figure 9) or macroscopic or microscopic gastrointestinal appearance following HSC depletion (Supplementary Figure 10). Specifically, there was no edema, necrosis, or inflammation in the bowel of either WT and TG mice. Complementary, intestinal decontamination reported same results regarding HSC depletion (data not shown), excluding the possibility for an altered gut permeability as a possible cause.

Functional consequences of HSC depletion

Having established a specific, reproducible method of HSC depletion, we next explored the functional impact of HSC loss on fibrosis, liver injury, and hepatic inflammation in the two models.

Attenuated hepatic fibrosis—Because activated HSCs are the main collagen-producing cell during liver injury, we assessed fibrosis by collagen morphometry following their depletion. Following 11 days of CCl_4+AA+GCV treatment, collagen deposition was significantly decreased in *GFAP-HSV-Tk* mice compared to WT animals as determined by Sirius Red/Fast Green staining and morphometry (Figure 4A). This finding could also be observed in mice treated with BDL+GCV (see Figure 4B).

Reduced hepatic injury—There was a significant diminution in the extent of liver necrosis after HSC depletion in TG by both fibrosis models based on histology and serum chemistry. Blinded pathologic scoring revealed significantly decreased scores for necrosis for both CCl_4+AA+GCV (Figure 5A) and BDL+GCV treated TG animals (Figure 5B), thus underscoring the applicability of this deletion approach to two mechanistic distinct fibrosis models. AST/ALT levels were significantly reduced in CCl_4+AA+GCV treated animals indicating less liver injury (Figure 6A). The same trend could be observed for BDL+GCV treated animals (Figure 6B) while no significant differences were observed in serum total billirubin or total protein (data not shown). Consistent with histological results there was a significantly reduced expression of HMGB1 (a marker of hepatic injury (18)) in TG animals

with HSC depletion (Supplementary Figure 11). The extent of hepatic injury (as assessed by histology scores for centrilobular necrosis, ballooning, serum AST/ALT levels) coincided temporally with the extent of HSC depletion in mice treated for 0, 4 and 7 days with CCl_4+AA+GCV, reinforcing the role of HSCs in provoking injury (Supplementary Figure 12).

To address potential sources of decreased liver damage, we analyzed a marker of lipid peroxidation, 4-hydroxy-2-nonenal (4-HNE) by immunoblotting in whole liver lysates from CCl_4+AA+GCV animals, which revealed a significant decrease in 4-HNE-modified proteins in TG mice undergoing HSC depletion (Figure 6C).

We also determined if HSC depletion can be maintained for up to one month by continuing a depletion treatment with reduced doses of CCl_4 and GCV in order to evaluate the impact on survival rates, non-liver effects, fibrosis and damage (treatment summarized in Supplemental Figure 1C). Consistent with previous results, there remained a statistically significant decrease in fibrosis (Figure 7A) and liver damage as assessed by histological necrosis scores (Figure 7B) and ALT levels (Figure 7C) in TG mice. Interestingly, an increase in ballooning degeneration was evident in TG mice whereas there was a decrease in centrilobular necrosis. There were no significant differences in overall survival or weight loss in TG or WT mice (data not shown).

Altered intrahepatic leukocyte population and intrahepatic cytokine expression—An initial screen using a cytokine bead array assay revealed induction of two key anti-inflammatory cytokines, IL-10 and IFN-γ in CCl_4+AA+GCV HSC depleted TG mice (Figure 8A), and of IL-10 but not IFN-γ in BDL+GCV treated TG mice (Figure 8B). No changes in IL-6 or TNF-α concentrations were observed (data not shown). To characterize possible sources of IL-10 and IFN-γ we analyzed intrahepatic leukocyte populations and performed polychromatic flow cytometry analysis. Dendritic cells, natural killer cells and $CD4^+$ and $CD8^+$ T cells, major potential sources of IFN-γ, were significantly increased in TG HSC depleted mice. Among immune cells that produce IL-10, both Tregs and $Ly6C^+/F4/80^+/CD11b+$ cells were significantly recruited to the liver during HSC depletion (Supplementary Figure 13).

Discussion

Ongoing efforts have attempted to target HSCs with cell-specific reagents as a potential diagnostic or therapeutic tool. Concomitantly, cell-specific depletion has been exploited in other cell types to establish their contribution to organ homeostasis (e.g, macrophages), with a few studies examining HSC depletion (2–5). To date, these investigations have reinforced the HSC's known role in fibrogenesis but have not expanded their repertoire of potential contributions to liver injury and inflammation. Gliotoxin, even when targeted to HSCs by coupling to antibodies to synaptophysin, could have broad actions *in vivo* on immune cells that have not been characterized thoroughly yet, for example by analyzing for macrophage markers other than $F4/80^+$ (e.g. CD68) or by FACS analysis of intrahepatic leukocytes (3, 4).

We report here a new murine model of HSC depletion that uncovers a previously unknown role in amplifying liver injury, using mice expressing the *HSV-Tk* gene driven by the mouse GFAP promoter. This system restricts cell depletion to proliferating HSCs, thereby uncovering the impact of only activated HSCs to liver injury and repair, because quiescent, non-proliferating HSCs are not affected.

Initial analyses confirmed reduced HSC proliferation (~50%) and increased apoptosis in isolated, cultured HSCs from TG mice when treated with GCV, consistent with previous studies utilizing the *HSV-Tk* `suicide gene' strategy (12), and mimicking the natural fate of HSC during resolution acute liver damage (19). Of note, approximately 70% of HSCs express GFAP (20), so that GCV-mediated killing affects the majority, but not all HSCs. Importantly, neither hepatocytes from either WT or TG mice, nor immortalized sinusoidal endothelial cells were depleted by the same treatment, reinforcing the cellular specificity of this model. Because GFAP-*HSV-Tk* is expressed in specific cells outside the liver (e.g., enteric glial cells) we excluded the possibility that the liver effects resulted from the loss of GFAP-expressing cells in other tissues or altered metabolism. Lethal effects of GCV (16) were reported after 14 days of continuous treatment with GCV (100 μg/g/d) via a subcutaneous pump in these mice. We therefore limited the GCV treatment to 11 days administered once daily i.p. Based on its pharmacokinetics, toxic serum levels of GCV are expected to be of a much shorter duration, therefore minimizing adverse effects. Indeed, we did not see increased lethality or mortality, or altered small bowel pathology with our treatment scheme.

Once in vivo HSC depletion was achieved, its functional impact was assessed by measuring markers of HSC activation. There was a dramatic decrease in α-SMA positive cells in TG mice undergoing HSC depletion, together with other markers of HSC proliferation (ie., β-PDGFR and collagen I), indicating that depletion affected those HSCs most critical to fibrogenesis and repair (i.e. activated HSCs). Of interest, CXCR4 expression was also decreased in TG mice undergoing HSC depletion. This cytokine receptor is another feature of activated HSCs, which also contributes to profibrogenic and proliferative responses (17).

The findings reinforce the rationale for therapeutic HSC depletion, albeit not necessarily by a suicide gene strategy. Moreover, not only was fibrosis reduced, but acute damage was attenuated, suggesting that depletion of activated HSCs could have dual salutary effects on both the amount of fibrosis and extent of injury. Correlated with attenuated injury was a reduction in 4-HNE consistent with decreased oxidant stress, although the source(s) of these pro-oxidants in both WT and TG mice are not clarified by our findings. Specifically, reduction in 4-HNE could reflect decreased release by HSCs because of their depletion, or loss of paracrine signals from HSCs to other cell types that generate 4-HNE, including hepatocytes or inflammatory cells. Moreover, 4-HNE interacts directly with JNK isoforms in human HSCs to stimulate pro-collagen type I expression and synthesis (21). Thus, reduced collagen production could also result from a feedback loop in which less 4-HNE leads to less JNK-mediated collagen expression. Of note, previous studies using gliotoxin did not uncover an impact of HSC depletion on injury (2, 5), possibly because effects of gliotoxin are not as specific, and concurrent effects of gliotoxin on other cell types might have attenuated the phenotype.

The mechanism of attenuated injury in the setting of HSC depletion is not fully clarified, but the increase in IL-10 and IFN-γ likely contribute to reduced injury, since these two cytokines both down-regulate HSC activation and fibrosis production (22). Polychromatic flow cytometry for intrahepatic immune cell populations revealed increased numbers of well known cellular sources of IL-10 (Tregs and monocytes) (23) as well as for IFN-γ (DC, NK, CD4+ and CD8+ T cells) (24). Specifically, the increase in Tregs along with an increase of IL-10, which unlike IFN-γ was evident in both HSC depletion models, indicates a potential role for Tregs in the attenuation of liver injury despite increased numbers of several immune cell populations in the absence of HSCs. Further studies to analyze these preliminary findings and to identify the responsible immune cell population by specific depletion studies *in vivo* are currently underway.

Importantly, injury was attenuated following HSC depletion not only in acute, but also in chronic injury (30 days after HSC depletion with continued CCl_4 and GCV) as well as in the BDL fibrosis model, indicating that the results are generalizable and not restricted to a single model of injury. Mice with HSC depletion after chronic injury all survived, attesting to the practicality of chronic HSC depletion with this strategy. Interestingly, the reduced injury in TG mice was associated with more hepatocyte ballooning, raising the prospect that ballooning degeneration but not necrosis could be beneficial, as ballooning has been previously proposed to indicate a better chance of cellular recovery after injury (25).

Our studies further suggest that HSCs (and not portal myofibroblasts, which reportedly not express GFAP (26) and are therefore not ablated in this model) are the major fibrogenic cell population in BDL-induced fibrosis consistent with an earlier study analyzing HSCs in different models by microarray (27).

In conclusion, we describe a new approach to HSC depletion that has confirmed the primacy of these cells in fibrosis production, but has also revealed an unexpected role in amplifying hepatocellular liver damage and decreasing protective cytokines. The model offers the prospect of exploring other features of liver homeostasis that may depend on HSCs, including their repopulation from extrahepatic sources and their contribution to hepatic regeneration and neoplasia.

Supplementary Material

Refer to Web version on PubMed Central for supplementary material.

Acknowledgments

We thank Drs. Virginia Hernandez Gea, and Feng Hong and Stephanie Gillespie for technical support, Dr. Vijay Shah for his generous donation of TSEC cells and Dr. Inma Castilla de Cortázar for her helpful advice.

Financial Support: Supported by funds from the Alfonso Martin Escudero Fundation (to J.P), the Deutsche Forschungsgemeinschaft (DFG) (to Y.L.) and NIH grants DK56621 & P20AA017067 (to S.L.F.).

List of Abbreviations

4-HNE	4-hydroxy-2-nonenal
α-SMA	alpha smooth muscle actin
GCV	ganciclovir
GFAP	glial fibrillary acidic protein
HMGB1	high-mobility group protein B1
HSC	hepatic stellate cell
HSV-Tk	herpes simplex virus-Thymidine kinase

References

1. Friedman SL. Hepatic Stellate Cells – Protean, Multifunctional, and Enigmatic Cells of the Liver. Physiological Reviews. 2008; 88:125–172. [PubMed: 18195085]
2. Orr JG, Leel V, Cameron GA, Marek CJ, Haughton EL, Elrick LJ, Trim JE, et al. Mechanism of action of the antifibrogenic compound gliotoxin in rat liver cells. Hepatology. 2004; 40:232–242. [PubMed: 15239107]

3. Ebrahimkhani MR, Oakley F, Murphy LB, Mann J, Moles A, Perugorria MJ, Ellis E, et al. Stimulating healthy tissue regeneration by targeting the 5-HT2B receptor in chronic liver disease. Nat Med. 2011; 17:1668–1673. [PubMed: 22120177]
4. Douglass A, Wallace K, Parr R, Park J, Durward E, Broadbent I, Barelle C, et al. Antibody-targeted myofibroblast apoptosis reduces fibrosis during sustained liver injury. J Hepatol. 2008; 49:88–98. [PubMed: 18394744]
5. Hagens WI, Olinga P, Meijer DK, Groothuis GM, Beljaars L, Poelstra K. Gliotoxin non-selectively induces apoptosis in fibrotic and normal livers. Liver Int. 2006; 26:232–239. [PubMed: 16448462]
6. Anselmi K, Stolz DB, Nalesnik M, Watkins SC, Kamath R, Gandhi CR. Gliotoxin causes apoptosis and necrosis of rat Kupffer cells in vitro and in vivo in the absence of oxidative stress: exacerbation by caspase and serine protease inhibition. J Hepatol. 2007; 47:103–113. [PubMed: 17466404]
7. Moolten FL. Tumor chemosensitivity conferred by inserted herpes thymidine kinase genes: paradigm for a prospective cancer control strategy. Cancer Res. 1986; 46:5276–5281. [PubMed: 3019523]
8. Moolten FL, Wells JM. Curability of tumors bearing herpes thymidine kinase genes transferred by retroviral vectors. J Natl Cancer Inst. 1990; 82:297–300. [PubMed: 2299679]
9. Qian C, Bilbao R, Bruna O, Prieto J. Induction of sensitivity to ganciclovir in human hepatocellular carcinoma cells by adenovirus-mediated gene transfer of herpes simplex virus thymidine kinase. Hepatology. 1995; 22:118–123. [PubMed: 7601402]
10. Fillat C, Carrio M, Cascante A, Sangro B. Suicide gene therapy mediated by the Herpes Simplex virus thymidine kinase gene/Ganciclovir system: fifteen years of application. Curr Gene Ther. 2003; 3:13–26. [PubMed: 12553532]
11. Zhang Y, Huang SZ, Wang S, Zeng YT. Development of an HSV-tk transgenic mouse model for study of liver damage. FEBS J. 2005; 272:2207–2215. [PubMed: 15853805]
12. Janoschek N, van de Leur E, Gressner AM, Weiskirchen R. Induction of cell death in activated hepatic stellate cells by targeted gene expression of the thymidine kinase/ganciclovir system. Biochem Biophys Res Commun. 2004; 316:1107–1115. [PubMed: 15044099]
13. Kountouras J, Billing BH, Scheuer PJ. Prolonged bile duct obstruction: a new experimental model for cirrhosis in the rat. Br J Exp Pathol. 1984; 65:305–311. [PubMed: 6743531]
14. Guo J, Hong F, Loke J, Yea S, Lim CL, Lee U, Mann DA, et al. A DDX5 S480A polymorphism is associated with increased transcription of fibrogenic genes in hepatic stellate cells. J Biol Chem. 2010; 285:5428–5437. [PubMed: 20022962]
15. Huebert RC, Jagavelu K, Liebl AF, Huang BQ, Splinter PL, Larusso NF, Urrutia RA, et al. Immortalized liver endothelial cells: a cell culture model for studies of motility and angiogenesis. Lab Invest. 2010
16. Bush TG, Savidge TC, Freeman TC, Cox HJ, Campbell EA, Mucke L, Johnson MH, et al. Fulminant jejuno-ileitis following ablation of enteric glia in adult transgenic mice. Cell. 1998; 93:189–201. [PubMed: 9568712]
17. Hong F, Tuyama A, Lee TF, Loke J, Agarwal R, Cheng X, Garg A, et al. Hepatic stellate cells express functional CXCR4: role in stromal cell-derived factor-1alpha-mediated stellate cell activation. Hepatology. 2009; 49:2055–2067. [PubMed: 19434726]
18. Liu A, Jin H, Dirsch O, Deng M, Huang H, Brocker-Preuss M, Dahmen U. Release of danger signals during ischemic storage of the liver: a potential marker of organ damage? Mediators Inflamm. 2010; 2010:436145. [PubMed: 21197406]
19. Elsharkawy AM, Oakley F, Mann DA. The role and regulation of hepatic stellate cell apoptosis in reversal of liver fibrosis. Apoptosis. 2005; 10:927–939. [PubMed: 16151628]
20. Geerts A. History, heterogeneity, developmental biology, and functions of quiescent hepatic stellate cells. Semin Liver Dis. 2001; 21:311–335. [PubMed: 11586463]
21. Parola M, Robino G, Marra F, Pinzani M, Bellomo G, Leonarduzzi G, Chiarugi P, et al. HNE interacts directly with JNK isoforms in human hepatic stellate cells. J Clin Invest. 1998; 102:1942–1950. [PubMed: 9835619]
22. Pinzani M, Marra F. Cytokine receptors and signaling in hepatic stellate cells. Semin Liver Dis. 2001; 21:397–416. [PubMed: 11586468]

23. Ma G, Pan PY, Eisenstein S, Divino CM, Lowell CA, Takai T, Chen SH. Paired immunoglobin-like receptor-B regulates the suppressive function and fate of myeloid-derived suppressor cells. Immunity. 2011; 34:385–395. [PubMed: 21376641]

24. Billiau A, Matthys P. Interferon-gamma: a historical perspective. Cytokine Growth Factor Rev. 2009; 20:97–113. [PubMed: 19268625]

25. Bergasa NV, Borque MJ, Wahl LM, Rabin L, Jones EA. Modulation of thioacetamide-induced hepatocellular necrosis by prostaglandins is associated with novel histologic changes. Liver. 1992; 12:168–174. [PubMed: 1406079]

26. Iwaisako K, Brenner DA, Kisseleva T. What's new in liver fibrosis? The origin of myofibroblasts in liver fibrosis. J Gastroenterol Hepatol. 2012; 27(Suppl 2):65–68. [PubMed: 22320919]

27. De Minicis S, Seki E, Uchinami H, Kluwe J, Zhang Y, Brenner DA, Schwabe RF. Gene expression profiles during hepatic stellate cell activation in culture and in vivo. Gastroenterology. 2007; 132:1937–1946. [PubMed: 17484886]

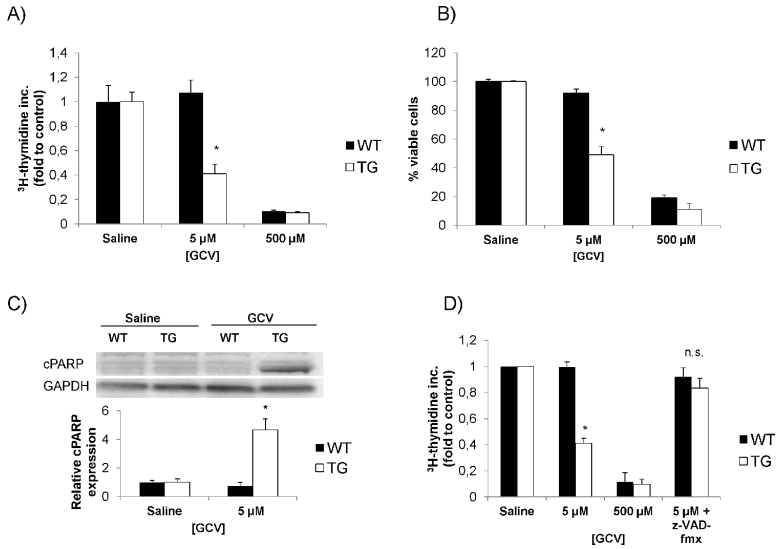

Figure 1. In vitro optimization of the GCV dose to provoke HSC depletion

(A) Characterization of HSC proliferation mediated by GCV in isolated HSC from TG mice as determined by ^{3}H-thymidine incorporation. A concentration of 5 μM GCV could specifically decrease TG HSC proliferation (B) Doses higher than 10 μM were toxic towards primary HSCs and hepatocytes from WT and TG mice as determined by trypan blue staining. (C) Immunoblotting for cleaved PARP expression in primary HSCs from both WT and TG mice. TG HSCs treated with GCV expressed more cleaved PARP consistent with increased apoptosis as mechanism for cell death. (D) Incubation with the pan-caspase inhibitor z-VAD-fmx abrogated the decrease in ^{3}H-thymidine incorporation of GCV on TG HSC. Data are mean values from three independent experiments. *p<0.05.

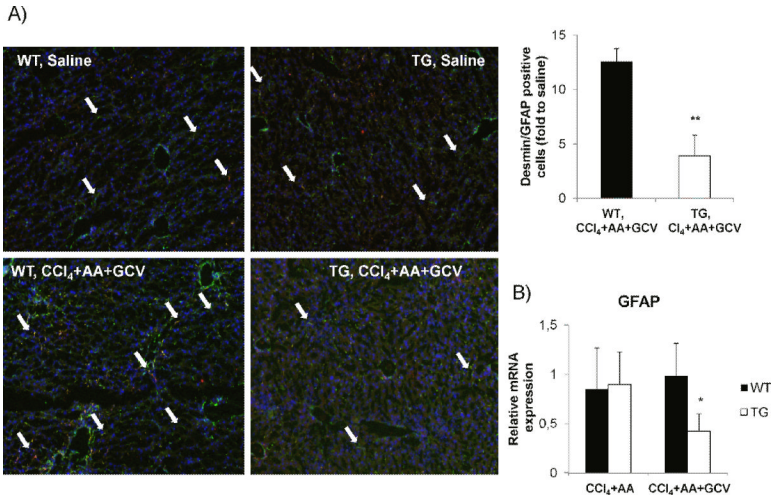

Figure 2. Validation of HSC depletion in vivo in TG mice treated with CCl_4+AA+GCV

(A) Reduction of desmin (green) and GFAP (red) positive cells, and merged images (yellow) by 65% ($p<0.01$) in TG mice treated with CCl_4+AA+GCV, compared to WT mice as assessed by dual-immunofluorescence. (B) Relative *GFAP* mRNA expression (by qPCR) demonstrates a significant reduction in TG mice undergoing HSC depletion. Data are mean values from three independent experiments normalized to saline-treated mice. GCV treatment (without CCl_4+AA) did not differ from saline treated group. Original magnification ×100. *$p<0.05$.

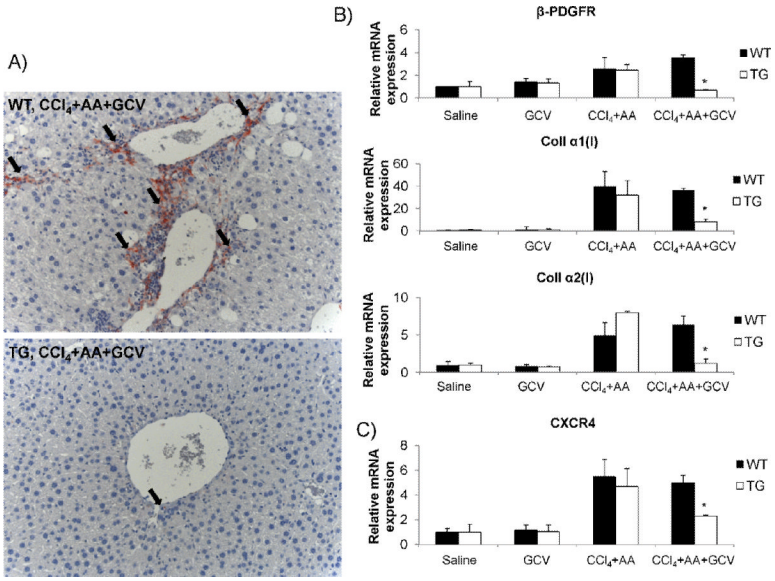

Figure 3. Reduced markers of HSC activation following HSC depletion

(A) Reduced α-SMA positive cells in TG mice undergoing HSC depletion as assessed by immunohistochemistry. (B) Relative mRNA expression genes associated with HSC activation (β-*PDGFR* and *collagen I*). There is a significant reduction of these markers in TG mice with HSC depletion. (C) Relative mRNA expression of *CXCR4* is reduced in TG mice undergoing HSC depletion. Original magnification ×200. *p<0.05.

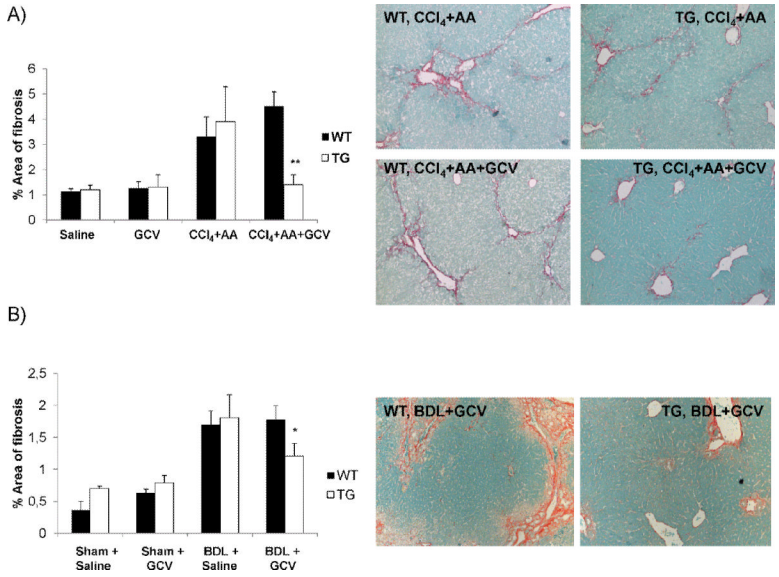

Figure 4. Attenuation of liver fibrosis in mice with HSC depletion

(A) Fibrosis content was quantified by Sirius Red/Fast Green staining and Bioquant computerized morphometry in (A) CCl4+AA+GCV treated mice as well as in (B) BDL +GCV treated mice. Original magnification ×100. *p<0.05; **p<0.01.

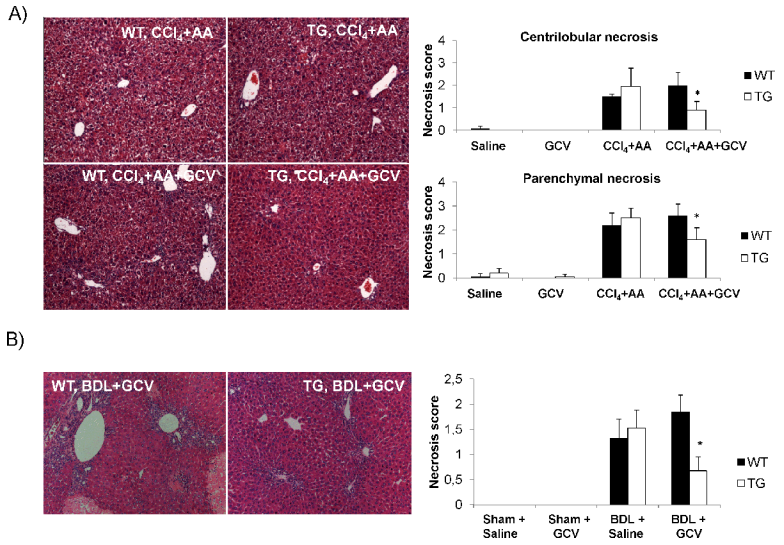

Figure 5. Reduced hepatic necrosis in mice with HSC depletion

(A) H&E staining and its histological scoring demonstrates a significant reduction in both centrilobular and parenchymal necrosis in TG mice undergoing HSC depletion by CCl_4+AA +GCV depletion treatment. (B) GCV treatment following BDL led to a consistent decrease in the extent of hepatic necrosis in TG mice undergoing HSC depletion. Original magnification ×100. *p<0.05.

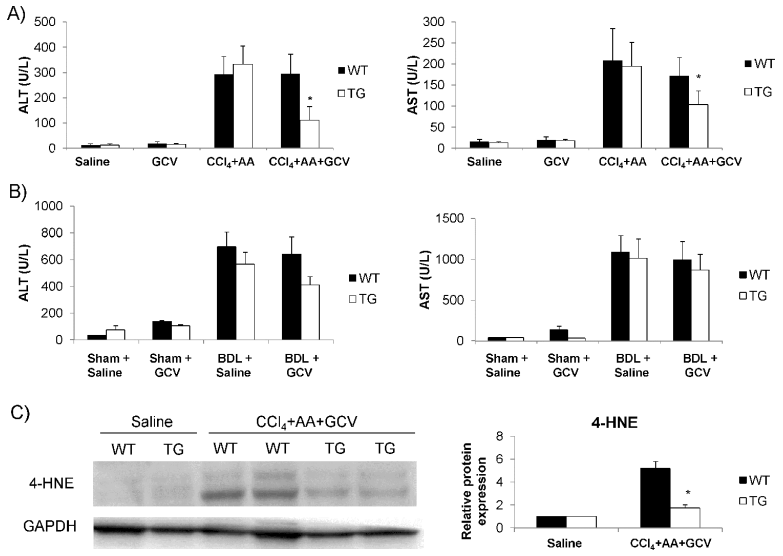

Figure 6. Reduced serum AST/ALT levels in mice with HSC and hepatic 4-HNE expression

ALT and AST levels are lower in TG mice treated with (A) CCl_4+AA+GCV and (B) in BDL+GCV treated animals compared to WT mice. (C) Protein from whole liver tissue was analyzed for 4-HNE expression by Western blot. Less oxidative damage was observed in TG mice undergoing HSC depletion than in WT mice. *p<0.05.

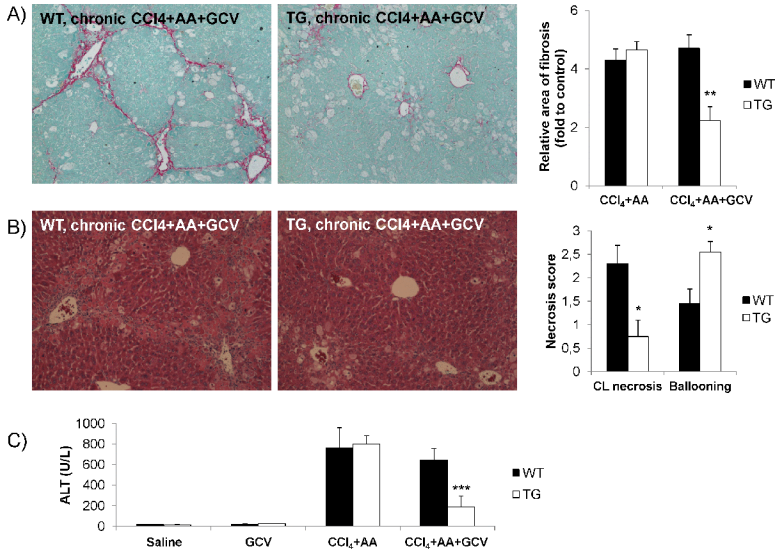

Figure 7. Effect of HSC depletion on chronic liver damage with CCl_4

(A) Fibrosis deposition is decreased in TG mice with HSC depletion undergoing chronic liver damage, compared to WT animals. Values are normalized to saline treated WT and TG mice. (B) H&E staining and histological scoring for hepatocellular necrosis and ballooning. TG mice displayed decreased necrosis compared to WT animals but increased ballooning. (C) TG mice undergoing HSC depletion had lower serum ALT levels compared to WT animals following chronic liver damage. CL, centrilobular. Original magnification ×100. *p<0.05, **p<0.01 and ***p<0.001.

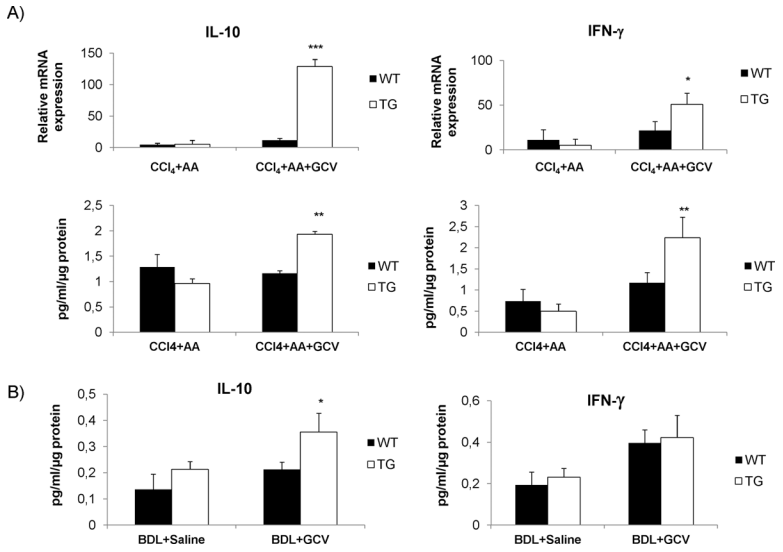

Figure 8. Increased IL-10 and IFN-γ in whole liver following HSC depletion

(A) Relative mRNA expression and protein concentration of IL-10 and IFN-γ were increased in TG mice undergoing HSC depletion by CCl_4+AA+GCV. (B) Protein concentrations for IL-10 and and IFN-γ in whole liver lysates of BDL+GCV treated mice. qPCR data are mean values from three independent experiments, normalized to saline-treated mice. GCV treatment (without CCl_4+AA) did not differ from saline treated group. *p<0.05, **p<0.01 and ***p<0.001.